RESEARCH ARTICLE

JCN RESEARCH IN SYSTEMS NEUROSCIENCE · THE JOURNAL OF COMPARATIVE NEUROLOGY WILEY

Functional alterations of retinal neurons and vascular involvement progress simultaneously in the *Psammomys obesus* model of diabetic retinopathy

Ahmed Dellaa[1] | Sihem Mbarek[1] | Rim Kahloun[2] | Mohamed Dogui[3] | Moncef Khairallah[2] | Imane Hammoum[1] | Narjess Ben Rayana-Chekir[4] | Ridha Charfeddine[5] | Pierre Lachapelle[6] | Rafika Ben Chaouacha-Chekir[1] (ID)

[1]Laboratory of Physiopathology, Food and Biomolecules, Higher Institute of Biotechnology of Sidi Thabet, BiotechPole Sidi Thabet, University of Manouba, Tunisia

[2]Department of Ophthalmology, Hospital of Fattouma Bourguiba, Monastir, Tunisia

[3]Department of Functional Explorations of the Nervous System, Hospital of Sahloul, Sousse, Tunisia

[4]Les Ophtalmologistes Associés de Sousse, Résidence Médicale Essalem, Place du Maghreb Arabe-Sousse, Tunisia

[5]UNIMED Laboratories, Sousse, Tunisia

[6]Department of Ophthalmology, Research Institute of the McGill University Health Centre, Montreal, Quebec, Canada

Correspondence
Rafika Ben Chaouacha-Chekir, Laboratory of Physiopathology, Food and Biomolecules, Higher Institute of Biotechnology of Sidi Thabet, BiotechPole Sidi Thabet, University of Manouba, Tunisia.
Email: rafika.chekir@gmail.com

Funding information
European Union

Abstract

To investigate the progression of diabetic retinopathy (DR) in a new diurnal animal model, we monitored clinically the DR in *Psammomys obesus* (*P. obesus*) during 7 months using electroretinography (ERG) and imaging techniques. After the onset of DR, all ERG components decreased progressively. In scotopic conditions, by 3-months of disease progression, the diabetic *P. obesus* displayed a significant decrease in amplitude of b-max, b-wave responses, and mixed b-waves. While mixed a-wave decreased between 4 and 7 months. Significant differences of OP2 appeared following 1 month of disease. In photopic conditions, we noticed a decrease in the a-wave at 2 months, while it took more than 5 months in b-wave amplitude. The photopic negative response (PhNR) and the i-wave amplitudes decreased following 4 and 5 months. OP1 and OP2 were the first to be altered and a significant decrease in the amplitude started after 3 months. Finally, 30 Hz-flicker and photopic S-cone were impaired after 2 and 3 months, respectively. The assessment of the eye fundus of the retina revealed an abnormal vascular architecture appeared at Months 6 and 7. In addition, we noticed exudates in the superior periphery of the retina at the same stage. The retina thickness showed a significant reduction at Month 7. Our results indicate that the clinical correlates of human DR are present in diabetic *P. obesus*. The depressed of ERGs, disruption of retinal architecture, and the appearance of exudates may reflect vascular and neuronal damage throughout the retina as are seen in the advanced stages of human DR.

KEYWORDS
diabetic retinopathy, early stage, *ERG*, neurodegeneration, *Psammomys obesus*

1 | INTRODUCTION

The vascular changes in diabetic retinopathy (DR) have been given much attention. But it is becoming clear that involvement of glial and neuronal cells may precede microvascular involvement (Verma et al., 2012). According to the clinical studies, DR is associated with multifactorial visual deficits (Hardy et al., 1992; Holm et al., 2007), including impaired electroretinographic (ERG) responses (Bearse et al., Bearse et al., 2004; Fortune et al., 1999; Palmowski, Sutter, Bearse, & Fung, Palmowski et al., 1997). In fact, functional alterations such as disturbances in color vision, contrast sensitivity, or anomalies of the electroretinogram have been reported to occur in

humans some time before the onset of clinical retinal abnormalities (Barber et al., 1998).

In animals and humans with diabetes, the most common ERG finding is that of reduced amplitudes and prolonged implicit times of the oscillatory potentials (OPs) (Kizawa et al., 2006; Kohzaki et al., 2008) and, in some cases, an altered photoreceptor response (Shirao & Kawasaki, 1998). The OPs are small amplitude, high-frequency wavelets, found on the rising slope of the b-wave and thought to signal amacrine cell activity (Wachtmeister, 1998). The early onset of OP anomalies suggests that these retinal interneurons might be more susceptible to diabetes more so given that the photoreceptor changes have been shown to be associated with the diabetes-induced lipid anomaly rather than to the hyperglycemia that also characterizes this condition (Kohzaki et al., 2008).

Of interest, anatomical studies also revealed some apoptosis of the ganglion cells in the early phase of diabetes, suggesting that ERG components tied to ganglion cell integrity could also be affected (Abu-El-Asrar et al., 2004; Barber et al., 1998), such as the photopic negative response (PhNR) (B. Li et al., 2005). In fact, in human and rodents affected with DR, the PhNR was previously shown to be altered (Kizawa et al., 2006). The PhNR was also shown to be reduced not only in DR but also in optic nerve diseases such as glaucoma and optic
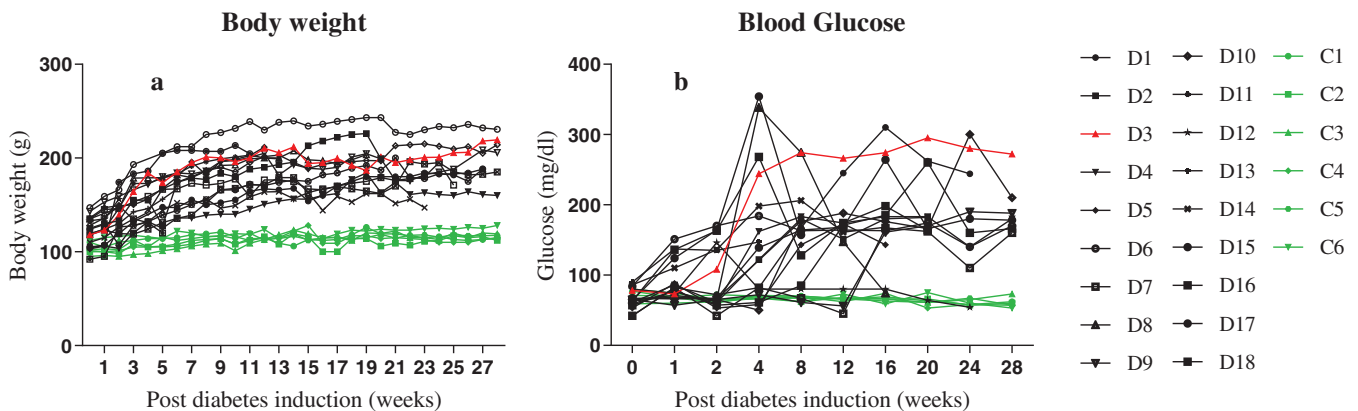

FIGURE 1 Individual body weight (a) and blood glucose (b) evolution in *P. obesus* for 7 months of diabetes induction. Diabetic (D): *n* = 18 (black line); control (C): *n* = 6 (green line); the red line in this and subsequent figures shows data for the rat D3, which is provided as an example throughout the period of experiments [Color figure can be viewed at wileyonlinelibrary.com]
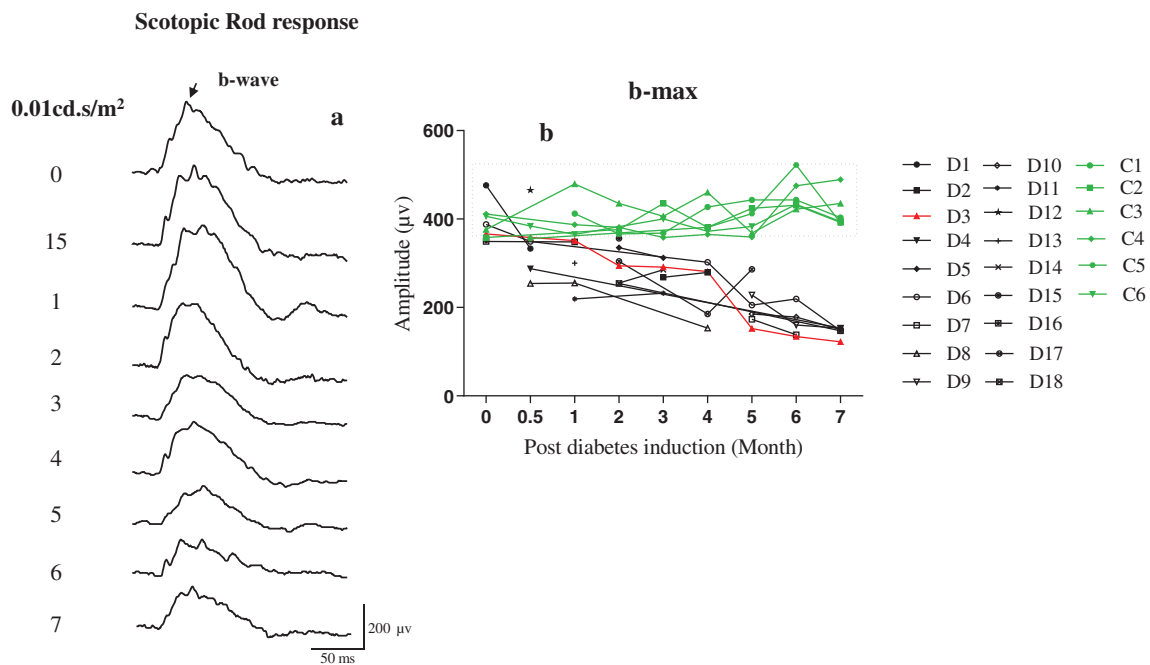

FIGURE 2 Scotopic electroretinography representative (a). Representative rod response stimulated using 0.01 cd.s/m² light intensity stimulation under scotopic condition in the dark adapted eye (b). Diabetic (D): *n* = 18; control (C): *n* = 6 (green curves) [Color figure can be viewed at wileyonlinelibrary.com]
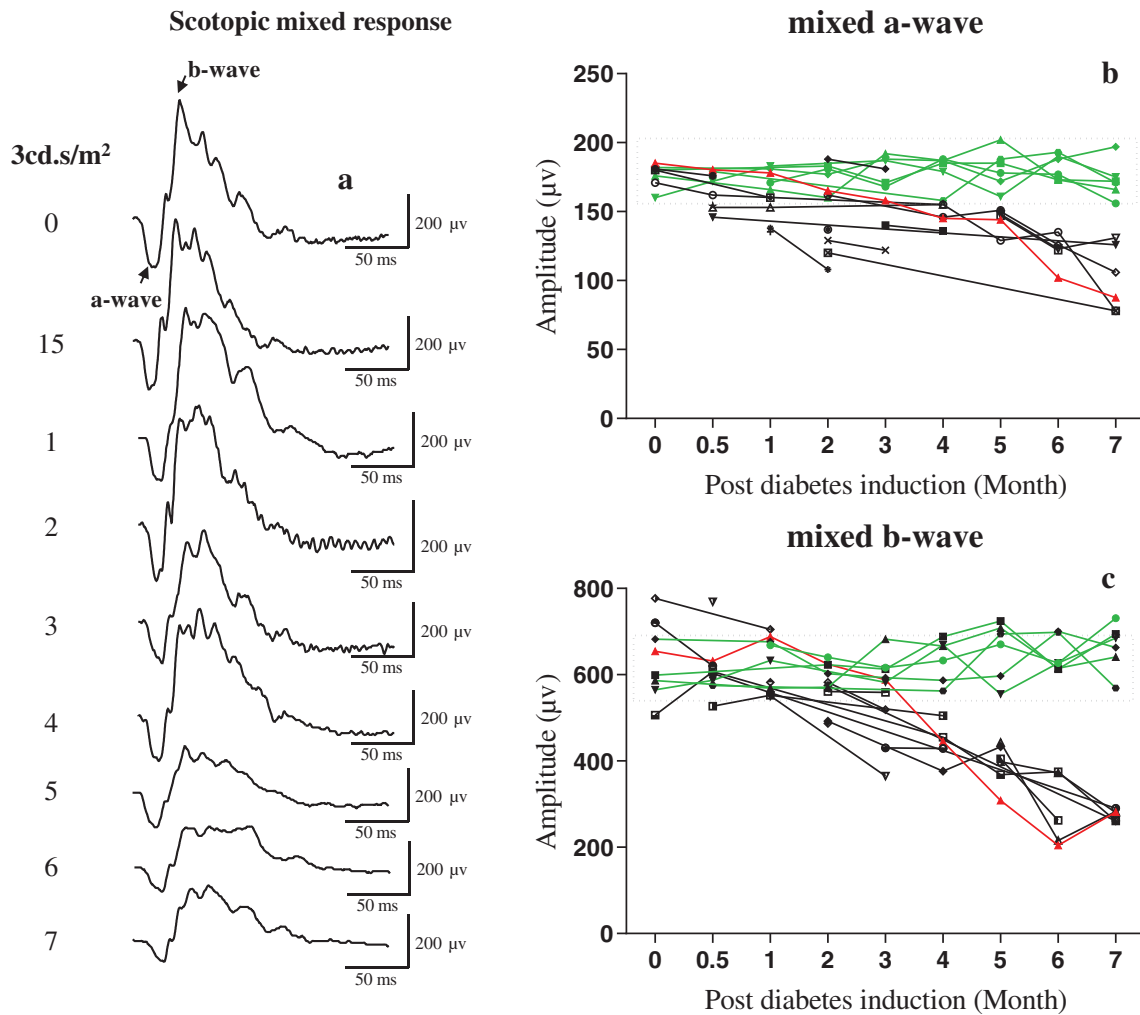
FIGURE 3 Scotopic electroretinography representative (a) representative rod response stimulated using 0.01 cd.s/m^2 light intensity stimulation under scotopic condition. (b) a-wave mixed response elicited at 3 cd.s/m^2 (c) b-wave mixed response in the dark adapted eye. Diabetic (D): n = 18; control (C): n = 6 (green curves) [Color figure can be viewed at wileyonlinelibrary.com]

nerve atrophy induced by trauma, compression, ischemia, or inflammation (Colotto et al., 2000; Gotoh et al., 2004; Kizawa et al., 2006; Rangaswamy et al., 2004; Viswanathan et al., 2001).

An increase in the apoptosis of retinal neurons as well as morphological alteration of the glial cells were also observed in primates and *P. obesus*, respectively, after 1 and 3 months of diabetes (Rangaswamy et al., 2004). Moreover, this loss of neuronal cells leads to a reduction in retinal thickness, which was demonstrated by optical coherence tomography in both human and rat (Hombrebueno et al., 2014; Sugimoto et al., 2005).

DR is classified into an early, nonproliferative stage, and a later, proliferative stage according to the degree of severity (Heng et al., 2013; Nentwich & Ulbig, 2015). One of the clinically detectable signs of DR is the increase in vascular permeability, due to a breakdown in the blood–retinal barrier, which causes macular edema (Cunha-Vaz et al., 1975). This is then followed by the development of vascular microaneurysms, deposition of lipoprotein exudates, and finally vascular proliferation (Aiello et al., 1998).

There are many rodent models of DR with varying degrees of similarity to human disease have been used in research of diabetes mellitus (DM) and its complications. The diurnal animal model *P. obesus* was introduced in the 1960s as a new model for studying diabetes (Haines et al., 1965; Schmidt-Nielsen et al., 1964). In its natural environment, this rodent consumes a low-calorie native plant, but in captivity, many individuals kept with a standard natural laboratory diet develop overweight with diabetes (Kaiser et al., 2005). The retina of *P. obesus* is rich in cones, which represent 41% of the total number of photoreceptors. The S cones represent an important proportion among the two types of cones present M and S (T. Saidi et al., 2011), which makes it an interesting model to study the pathologies related to the cones which characterize the central retina in humans. Type 2 diabetes (T2D), induced after treatment of 7 months with a high-calorie diet, affects neuronal, glial, vascular tissues as well as the composition of the vitreous of the retina (Saïdi et al., 2011).

In a previous manuscript (Dellaa et al., 2018), we reported ERG findings in *P. obesus* that had been affected with diabetes for

TABLE 1 ERG components for control and diabetic *Psammomys obesus*

ERG parameters (µv)	Day 0 Control	Day 0 Diabetic	Day 0 p-value	Day 15 Control	Day 15 Diabetic	Day 15 p-value	Month 1 Control	Month 1 Diabetic	Month 1 p-value	Month 2 Control	Month 2 Diabetic	Month 2 p-value	Month 3 Control	Month 3 Diabetic	Month 3 p-value
Rod response	337.75 ± 28.28	394.65 ± 28.24	.34	349.9 ± 3.41	324.43 ± 41.62	.85	350.75 ± 4467	283.24 ± 19.92	.41	34.450 ± 24.76	344.5 ± 24.76	.6	39.340 ± 13.84	29.620 ± 25.69	.03*
Scotopic b-wave	608 ± 25.64	685.5 ± 73.91	.48	581 ± 3.46	597.68 ± 20.53	.28	612.75 ± 25.93	619.60 ± 33.21	.90	599.00 ± 19.56	599.00 ± 19.56	.17	517.20 ± 22.68	510.20 ± 48.60	.015*
Scotopic a-wave	172 ± 7.43	179.25 ± 2.95	.57	168 ± 5.77	160.23 ± 7.53	.42	174.00 ± 4.14	155.28 ± 8.96	.6	175.25 ± 4.27	175.25 ± 4.27	.25	179.80 ± 5.91	144.40 ± 13.05	.63
Scotopic b–/a- ratio	3.54 ± 0.12	3.81 ± 0.38	.68	3.47 ± 0.24	3.94 ± 0.26	.42	3.52 ± 0.10	4.01 ± 0.17	.06	10.47 ± 0.78	3.79 ± 0.31	.47	2.88 ± 0.09	3.58 ± 0.31	.03*
OP1	27.79 ± 1.57	26.96 ± 3.21	.9	27.80 ± 1.83	25.48 ± 1.80	.41	27.96 ± 1.58	22.87 ± 3.10	.24	28.37 ± 1.51	14.43 ± 2.86	.008**	29.15 ± 2.55	12.15 ± 0.76	.015*
OP2	101.52 ± 6.85	122.23 ± 8.53	.17	118.85 ± 4.1	125.51 ± 10.57	.45	136.67 ± 8.21	93.35 ± 14.26	.04*	125.31 ± 6.16	98.85 ± 12.37	.01*	132.56 ± 12.84	76.92 ± 13.03	.01*
OP3	87.44 ± 3.33	117.87 ± 6.87	.009**	108.48 ± 5.12	117.71 ± 11.06	.69	120.17 ± 8.32	89.60 ± 16.78	.24	115.33 ± 7.45	119.86 ± 11.30	.73	120.93 ± 10.63	99.32 ± 20.94	.11
OP4	46.72 ± 4.46	58.15 ± 4.14	.17	57.88 ± 6.52	57.38 ± 5.69	.9	61.58 ± 4.54	63.42 ± 11.44	.79	61.21 ± 6.61	55.88 ± 8.76	.9	58.73 ± 5.73	53.42 ± 13.62	.11
Photopic a-wave	31.26 ± 1.03	31.12 ± 1.29	.88	31.3 ± 1.36	31.08 ± 1.50	.66	31.07 ± 0.89	27.72 ± 1.66	.30	31.17 ± .86	24.83 ± 0.85	.002**	32.43 ± 1.40	24.73 ± 0.90	.009**
Photopic b-wave	323.28 ± 13.5	461.62 ± 57.58	.15	323.4 ± 19.4	359.66 ± 15.28	.60	324.73 ± 17.86	325.58 ± 22.80	.96	324.12 ± 18.19	325.75 ± 17.83	.53	325.55 ± 15.67	225.50 ± 41.55	.17
Photopic b–/a- ratio	10.43 ± 0.66	14.65 ± 1.58	.06	11.02 ± 0.93	11.78 ± 0.97	.69	10.51 ± 0.69	11.81 ± 0.63	.32	3.41 ± 0.04	13.25 ± 1.01	.06	2.88 ± 0.09	9.13 ± 2.17	.47
i-wave	29.98 ± 3.12	28.27 ± 2.46	.71	29.6 ± 2.08	41.2 ± 7.88	.55	28.68 ± 1.41	28.76 ± 4.43	.09	28.78 ± 3.15	15.17 ± 4.26	.12	27.92 ± 4.33	15.67 ± 5.56	.11
PhNR	87.41 ± 5.56	97.07 ± 7.14	.47	87.36 ± 5.57	80.08 ± 6.46	.50	87.57 ± 5.93	86.48 ± 5.10	.93	87.12 ± 7.53	72.33 ± 6.26	.06	89.76 ± 5.67	68.00 ± 2.39	.05
OP1	24.94 ± 1.01	23.89 ± 1.69	.6	24.91 ± 1.8	23.64 ± 2.14	.37	25.31 ± 1.36	26.87 ± 0.53	.32	25.48 ± 1.17	21.26 ± 2.24	.07	23.47 ± 1.07	16.26 ± 1.37	.01*
OP2	50.20 ± 2.77	45.41 ± 1.39	.009**	50.11 ± 2.25	46.95 ± 1.92	.008**	95.03 ± 2.86	66.08 ± 2.77	.008**	50.16 ± 2.34	55.16 ± 5.29	.82	46.15 ± 3.40	31.95 ± 8.33	.03*
OP3	55.85 ± 3.98	53.51 ± 4.2	.6	54.95 ± 3.47	46.75 ± 2.9	.81	74.65 ± 3.38	91.92 ± 3.88	.17	58.36 ± 4.02	78.51 ± 10.91	.16	50.92 ± 4.62	59.03 ± 15.73	.47
OP4	41.47 ± 3.15	41.47 ± 2.54	.9	41.86 ± 2.85	37.97 ± 3.46	.008**	41.16 ± 2.62	59.06 ± 4.94	.47	40.82 ± 3.02	60.30 ± 5.80	.17	41.36 ± 2.79	47.00 ± 13.04	.11
30-Hz flicker	304.3 ± 16.56	387.8 ± 28.92	.16	302.2 ± 19.7	289.2 ± 21.88	.88	302.33 ± 20.62	340.63 ± 20.29	.9	305.87 ± 24.9	262.90 ± 21.03	.009**	301.63 ± 18.65	240.75 ± 26.37	.06
Photopic S-cone	42.83 ± 2.22	56.65 ± 9.47	.60	42.86 ± 2.1	33.73 ± 4.14	.02*	42.28 ± 3.20	41.74 ± 3.96	.05	42.01 ± 2.58	37.27 ± 2.41	.06	41.47 ± 2.24	33.48 ± 4.37	.009**

ERG parameters (µv)	Month 4 Control	Month 4 Diabetic	Month 4 p-value	Month 5 Control	Month 5 Diabetic	Month 5 p-value	Month 6 Control	Month 6 Diabetic	Month 6 p-value	Month 7 Control	Month 7 Diabetic	Month 7 p-value
Rod response	218.40 ± 27.47	218.40 ± 27.47	.004**	398.17 ± 13.59	242.83 ± 32.69	.002**	454.33 ± 15.47	242.83 ± 32.69	.009**	400.67 ± 26.16	145.33 ± 4.79	.002*
Scotopic b-wave	466.08 ± 28.02	466.08 ± 28.02	.0043**	672.50 ± 33.11	435.00 ± 40.85	.002**	646.67 ± 16.72	435.00 ± 40.85	.004**	663.83 ± 22.65	276.12 ± 4.95	.002**
Scotopic a-wave	152.26 ± 12.06	152.26 ± 12.06	.004**	179.17 ± 7.16	138.33 ± 11.96	.002**	182.33 ± 3.68	138.33 ± 8.40	.002**	172.83 ± 5.55	105.62 ± 11.14	.002**
Scotopic b–/a- ratio	3.10 ± 0.16	3.51 ± 0.09	.05	3.75 ± 0.06	3.14 ± 0.18	.03*	3.55 ± 0.05	2.18 ± 023	.004**	3.86 ± 0.20	2.75 ± 0.25	.008**

(Continues)

TABLE 1 (Continued)

ERG parameters (µv)	Month 4			Month 5			Month 6			Month 7		
	Control	Diabetic	p-value	Control	Diabetic	p-value	Control	Diabetic	p-value	Control	Diabetic	p-value
OP1	28.73 ± 2	13.23 ± 1.40	.009**	29.15 ± 2.09	19.77 ± 4.43	.01*	29.46 ± 5.64	15.34 ± 2.43	.01*	29.69 ± 2.44	15.27 ± 2.06	.002**
OP2	136 ± 10	38.88 ± 6.97	.009**	136.75 ± 5.65	53.18 ± 12.36	.009**	127.72 ± 2.28	41.27 ± 10.32	.007**	137.33 ± 8.20	23.18 ± 1.71	.002**
OP3	119.76 ± 27.7	74.57 ± 22.97	.009**	120.77 ± 11.33	50.13 ± 9.13	.009**	107.35 ± 15.69	34.82 ± 6.53	.007**	121.92 ± 11.29	38.97 ± 5.76	.002**
OP4	62.82 ± 6.81	37.77 ± 11.30	.17	62.52 ± 4.23	28.25 ± 6.46	.009**	42.20 ± 7.03	18.26 ± 2.41	.007	63.05 ± 5.50	23.66 ± 3.98	.008
Photopic a-wave	25.22 ± 1.19	25.22 ± 1.19	.002**	31.25 ± 1.06	22.36 ± 0.77	.004**	32.53 ± 1.99	22.00 ± 1.81	.004**	29.10 ± 0.51	18.87 ± 0.41	.002**
Photopic b-wave	281.96 ± 13.91	281.96 ± 13.91	.17	342.92 ± 25.21	201.60 ± 19.61	.17	14.73 ± 0.23	153.36 ± 4.92	.004**	326.42 ± 15.76	153.35 ± 21.04	0.002**
Photopic b−/a− ratio	11.42 ± 1.22	10.18 ± 1.05	.53	11.13 ± 1.03	9.09 ± 0.88	.08	11.39 ± 1.39	7.15 ± 0.57	.08	11.21 ± 0.49	8.14 ± 1.11	.02
i-wave	26.78 ± 6.21	26.78 ± 6.21	.17	34.33 ± 3.52	19.06 ± 2.84	.08**	36.08 ± 4.15	6.80 ± 1.46	.004**	27.20 ± 4.58	11.82 ± 0.50	.002**
PhNR	67.64 ± 5.57	67.64 ± 5.57	.03*	87.48 ± 7.74	52.86 ± 9.45	.01*	109.75 ± 13.88	37.80 ± 4.73	.004**	85.32 ± 8.01	39.13 ± 4.96	.008**
OP1	17.77 ± 2.89	25.65 ± 1.86	.007**	26.54 ± 2.45	16.28 ± 2.59	.002**	30.24 ± 2.12	7.94 ± 1.31	.004**	25.29 ± 1.61	11.13 ± 0.61	.002**
OP2	32.57 ± 6.66	43.95 ± 1.43	.007**	45.33 ± 4.79	27.64 ± 6.43	.002**	43.26 ± 2.12	15.63 ± 3.86	.004**	48.32 ± 3.67	15.24 ± 1.66	.002**
OP3	39.87 ± 11.85	46.17 ± 3.46	.05	50.38 ± 3.03	32.90 ± 8.26	.05	49.95 ± 3.69	18.17 ± 3.65	.08*	53.18 ± 4.26	17.86 ± 3.05	.002**
OP4	31.21 ± 10.36	26.63 ± 3.32	.15*	31.13 ± 1.69	28.18 ± 6.90	.15*	29.76 ± 4.40	16.59 ± 1.76	.13	39.23 ± 3.20	15.55 ± 2.47	.002**
30-Hz flicker	215.50 ± 11.02	215.50 ± 11.02	.004**	270.72 ± 11.72	157.02 ± 23.68	.004**	298.58 ± 11.76	113.80 ± 7.62	.004**	295.23 ± 20.70	99.47 ± 4.26	.002**
Photopic S-cone	30.52 ± 2.13	30.52 ± 2.13	.004**	40.70 ± 1.98	30.36 ± 4.92	.002**	44.82 ± 5.42	23.36 ± 1.24	.002**	40.75 ± 2.08	24.73 ± 3.28	.002**

Note: Data are expressed as the mean ± SEM. Amplitude is in microvolts (µV).
*$p \leq .05$. **$p \leq .01$.

7 months. This study revealed a significant decrease of all ERG components in both scotopic and photopic conditions. The present report will focus on the early manifestation observed in the retinal structure and function in the diet-induced T2D of *P. obesus* and how these changes progressed over the 7-month period.

2 | MATERIALS AND METHODS

2.1 | Animals

Animals were captured in the Bou-Hedma National Park, which is a semi-desertic area of southern Tunisia, in accordance with the national regulations on the treatment of wildlife. Following capture, each *P. obesus* was held in quarantine for adaptation prior to experimentation. *P. obesus* were housed under laboratory standard conditions of 12D/12L light cycle, temperature, and relative humidity were set at 24°C ± 1°C and 70% ± 5%. Food and water were provided ad libitum.

Six control and 18 diabetic animals were used for this experiment. The control group received a natural hypocaloric (0.4 kcal/g wet weight) vegetable diet, that is, halophilic plants (Chenopodiaceae), rich in water and mineral salts and the diabetic group received a standard laboratory rat enriched chow feed (4 kcal/g wet weight). Body weight was monitored weekly and blood glucose was measured every month at the same time during the fasting for the entire duration of the study.

All procedures adhered to the ARVO Statement for the Use of Animals in Ophthalmic and Vision Research and protocols were approved by the local biomedical ethic committee at the Pasteur Institute of Tunis (2016/11/E/ISBST/V1). *P. obesus* were captured according to the rules authorization of Tunisian Agriculture Ministry (ref. 2016/1693).

2.2 | Clinical investigation

2.2.1 | Electroretinography

ERGs were recorded using a Metrovision system (France) following 15 days, 1, 2, 3, 4, 5, 6, and 7 months after the onset of diabetes according to a method previously described by us (Dellaa et al., 2016; Dellaa et al., 2018). The animals were anesthetized with an intraperitoneal injection of ketamine (120 mg/kg), the pupils dilated with tropicamide (25 mg/5 ml; UNIMED, Tunisia) and the cornea anesthetized with eye drops of 0.5% Alcaine (Bausch & Lomb, France). The retinal activity was recorded with a DTL electrode (X-static silver coated conductive nylon yarn, Sauquoit Industries, Scranton, PA) retained on the cornea with tear gel (Lacryvisc, Carbomer 974 P, Alcon), while the reference and ground electrodes were placed on the forehead and tail, respectively. Scotopic ERGs were recorded following overnight dark adaptation while photopic ERGs were obtained after 10 min of light-adaptation. Photopic and scotopic ERGs were
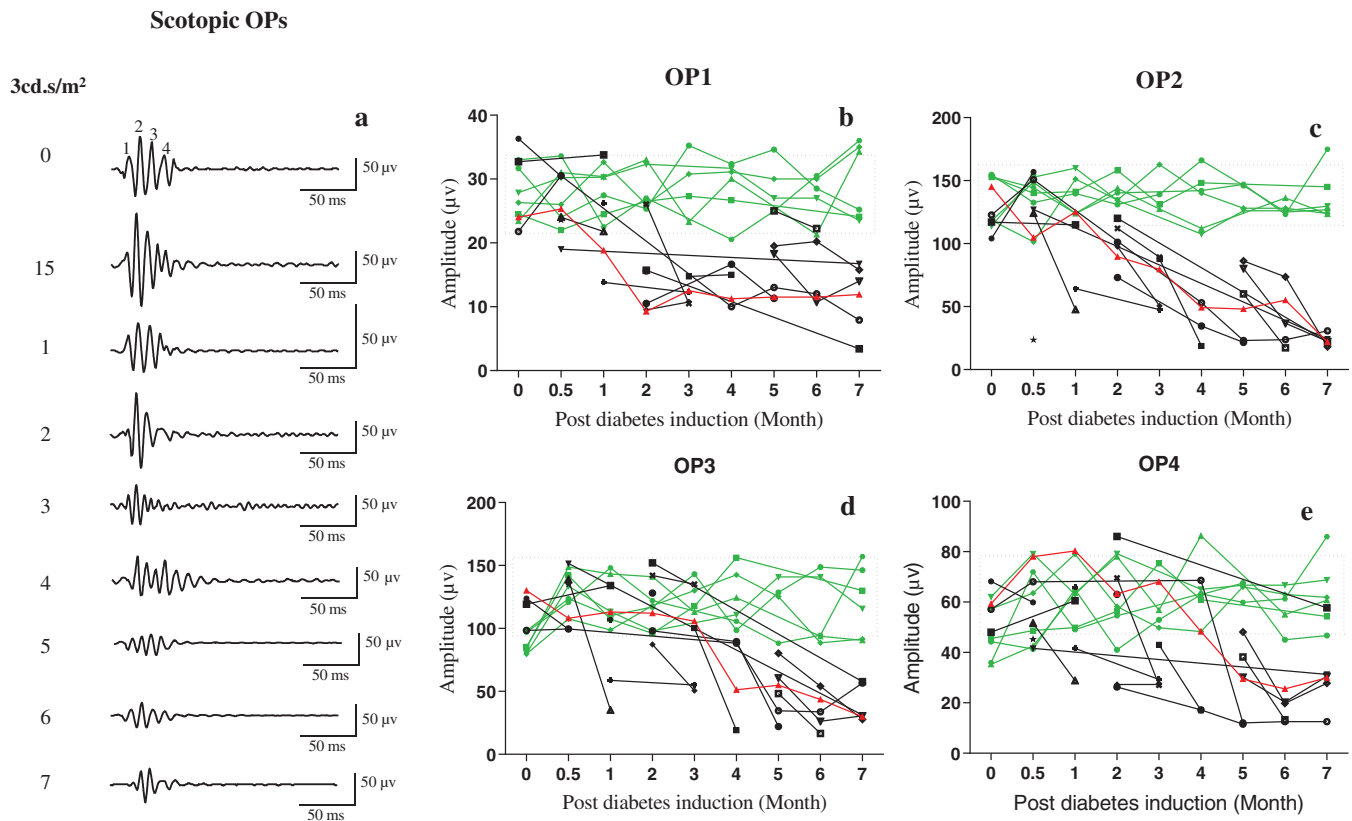
FIGURE 4 Oscillatory potentials, isolated by the band-pass filter, recorded from control and diabetic *P. obesus* in response to a flash of 3 cd.s/m^2 (a). OP1: (b); OP2: (c); OP3: (d); and OP4: (e). (D) Diabetic: *n* = 18; (C) control: *n* = 6 (green curves) [Color figure can be viewed at wileyonlinelibrary.com]

recorded following the Standards of the International Society for Clinical Electrophysiology of Vision (ISCEV) (McCulloch et al., 2015).

All recordings were obtained in a dark room to ensure complete dark adaptation. The scotopic ERG signals were amplified (×12,500) and filtered (1–1200 Hz). Scotopic responses were evoked to flash stimuli of 0.01 cd.s/m^2 and 3 cd.s/m^2. The oscillatory potentials were extracted by Fourier transform using an 80–200 Hz bandwidth. The animals were then light adapted to a rod-desensitizing background of 30 cd/m^2 for 10 min following which, photopic ERGs were evoked to flashes of 3 cd.s/m^2 in intensity. A 30-Hz flicker response was also obtained using the same flash intensity and background. The S-cone response was also obtained with the use of a purple flash (414 nm) stimulus of 0.0045 cd.s/m^2 in intensity delivered against a red-orange (595 nm) background of 150 cd/m^2 to suppress the contribution of rods and M cones.

Data analysis included the measurement of implicit times and amplitudes of ERG components (i.e., a-, b-, i- and S-cone waves, PhNR, flicker, and OPs). The amplitude of the a-wave was measured from the baseline to the first negative deflection, the b-wave from the trough of the a-wave to positive peak, the i-wave (Rosolen et al., 2004) from the trough following the b-wave peak to the peak of the i-wave, the PhNR from baseline to negative trough following the i-wave, the 30 Hz flicker from the trough to the peak, the analysis of the OPs was measured individually for the OP1-OP4 from the trough to the peak, and the S-cone was quantified as the b-wave amplitude. All peak times were measured from the flash onset to the peak of each component.

2.2.2 | In vivo imaging

Confocal scanning laser ophthalmoscopy

All imaging techniques were obtained after ERG recordings. Animals were anesthetized and their pupils dilated. Fundus images of right retinas were taken first by confocal scanning laser ophthalmoscopy, then fundus fluorescein angiography was observed after intraperitoneal fluorescein injection of 5 ml/kg of 2% fluorescein sodium dye solution (Alcon).

Optical coherence tomography imaging

Animals were anesthetized and their pupils dilated as described above. Spectral domain optical coherence tomography (SD-OCT) imaging was done using a Topcon 3D OCT-2000 system. Maps of retinal thickness were quantified and averaged from the pseudo-macula region using the proprietary software package.

2.3 | Data analysis

During the whole experiment, we used 24animals. Six diabetic animals were chosen randomly from the group on a high-calorie diet and six controls were used in each stage from 15 days to 7 months. Data sets were represented as mean ± standard error of mean (SEM). Comparisons between groups were made using the Mann–Whitney test. Differences were considered statistically significant when the *p* values were less than .05. All
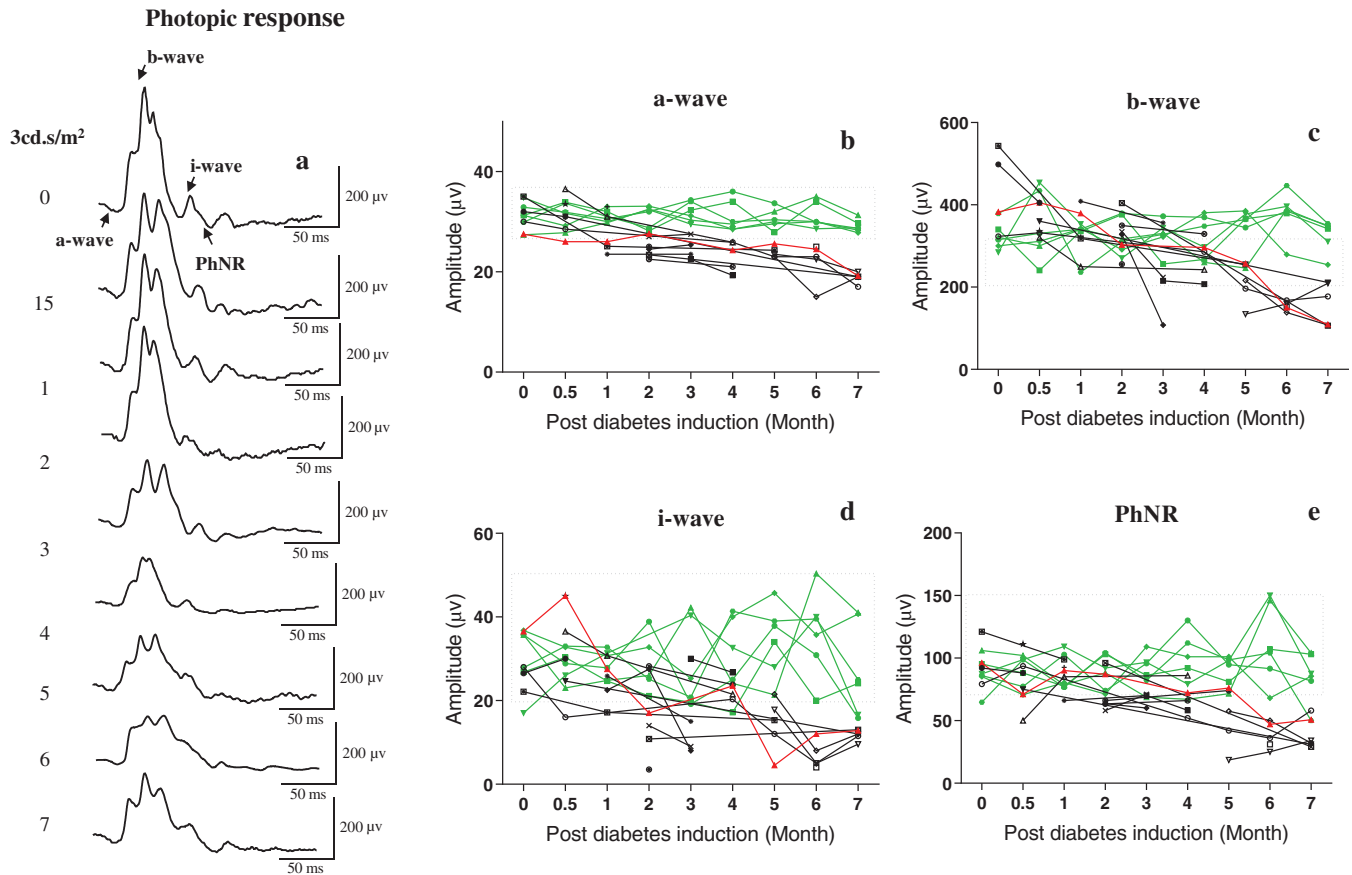
FIGURE 5 Photopic cone response at 3 cd.s/m² after 10 min light adaptation with 30 cd.s/m² background (a). (b) a-wave, (c) b-wave, (d) i-wave, (e) photopic negative response (PhNR). (D) Diabetic: *n* = 18; (C) control: *n* = 6 (green curves) [Color figure can be viewed at wileyonlinelibrary.com]

statistical analyses were performed with GraphPad Prism (GraphPad Software Inc., San Diego).

3 | RESULTS

To better track the ERG results and the medical imaging for the whole period from Day-0 to Month-7 and to have a credible assessment of the results, we are showing all the individual data. As exemplified at Figure 1 (a), during the experimental period, diabetic *P. obesus* progressively gained weight (some even doubled their weight) compared to the controls, whose body weight appeared to be more stable. This gradual change in body weight was also accompanied by a significant increase 4-fold in glycemia as witnessed with the data reported at Figure 1(b) compared to control *P. obesus* whose glycemia remained stable throughout. Of note, there was no evidence of cataract formation in either group.

3.1 | Assessment of the retinal function with the ERG

3.1.1 | Scotopic condition

Representative scotopic ERG waveforms (evoked to flashes of 0.01 cd.s/m² and 3 cd.s/m²) recorded from diabetic *P. obesus* at

selected time intervals following the onset of diabetes induction are shown with Figures 2(a) and 3(a), respectively. Group data are graphically reported at Figures 2(b) and 3(b,c) as well as in Table 1. Table 1 along with Figures 2 and 3 show that the amplitudes of the different ERG waveforms gradually decreased with the disease progression. For example, while in the early phase of the disease, there were no significant amplitude differences measured in scotopic responses, by 3-months of disease progression, the diabetic *P. obesus* displayed a significant decrease in amplitude of b-max, b-wave responses, and mixed b-wave (*p* = .03, *p* = .015, and *p* = .03), respectively (Figures 2 and 3(c) and Table 1). The mixed a-wave decreased dramatically (*p* = .001) between 4 and 7 months (Figure 3(b)).

Figure 4 showed the scotopic OP recordings obtained at different stages of diabetes. Amplitude measurements are reported in Table 1. Although there were no statistical differences noted at baseline between control and diabetic OPs, significant differences appeared following 1 month of disease for OP2 (Table 1, Figure 4(c) only. By 2 months, OP1 and OP2 were significantly reduced compared to control and after 5 months of the disease, the amplitude of all the OPs was significantly reduced (*p* = .01; .009; .009 and .009, respectively) in diabetic *P. obesus* (Figure 4, Table 1).

b/a-wave ratio shows a significant decrease at Month 3 (Table 1; *p* = .003), while the ratio returned to normal at Month 4 and then
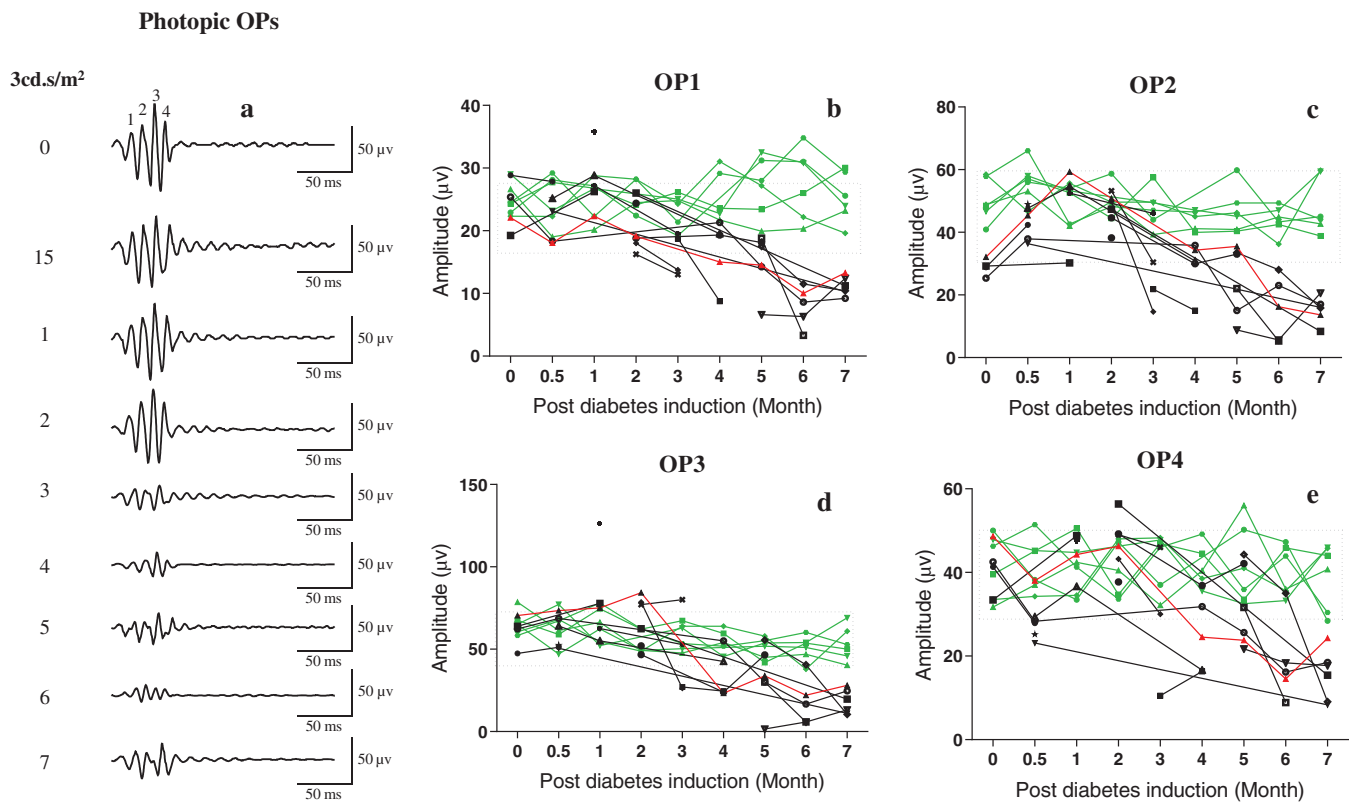
FIGURE 6 Photopic oscillatory potentials, isolated by the band-pass filter, recorded from control and diabetic *Psammomys obesus* in response to a flash of 3 cd.s/m². (a); OPs: (b): OP1, (c): OP2 (d): OP3, and (e): OP4. (D) Diabetic: *n* = 18; (C) control: *n* = 6 (green curves) [Color figure can be viewed at wileyonlinelibrary.com]

decreased significantly from Month 5 (*p* = .05). No difference was noticed for the photopic b/a-wave ratio.

3.1.2 | Photopic condition

As exemplified at Figure 5 and Table 1, the different components (a--wave, b-wave, i-wave, and PhNR) of the photopic ERG response were differently altered with the progression of the DR disease process. A significant decrease (*p* = .002) of the a-wave amplitude (Table 1, Figure 5(b)) was first noticed 2 months after the onset of diabetes, while it took more than 5 months before noticing a significant reduction (*p* = .017) in b-wave amplitude. The i-wave (Table 1, Figure 5(d)) and the PhNR (Table 1, Figure 5(e)), which reflect the function of ganglion cells, both saw their amplitude decrease following 4 and 5 months of disease progression, respectively (Table 1, Figure 5(d,e)).

The four major photopic oscillatory potentials (Table 1, Figure 6(a)), were differently impaired with the progression of the DR disease process. OP1 and OP2 (Figure 6(b,c)) were the first to be altered and a significant decrease in the amplitude started after 3 months of the onset of DR (Table 1, Figure 6(b,c)). By the sixth month, the amplitudes of OP3 and OP4 also became significantly reduced (*p* = .008) (Table 1, Figure 6(d,e)). Finally, the amplitudes of 30 Hz-flicker response (Figure 7(c)) and photopic S-cone (Figure 7(d)) were also significantly

impaired in diabetic animals after 2 and 3 months of diabetes induction, respectively (*p* = .009) (Table 1).

3.2 | Assessment of retinal thickness by OCT

We first took images by OCT, eye fundus and angiography in diabetic *P. obesus* at various stages of diabetes induction. The OCT in vivo was used to assess the retinal thickness and show the distinctive retina layer sections. Retinal thickness was unchanged during the first 6 months of diabetes. Only at Month 7, the OCT showed a significant decrease in the retinal thickness (*p* = .001) of diabetic rats when compared with controls (Figure 8, Table 2). Moreover, the OCT section showed hard exudates in retinal layer (bold red arrows).

3.3 | Assessment of retinal vascularization by eye fundus and angiography

The blood vessel architecture was analyzed by eye fundus (Figure 9) and angiography in *P. obesus* during the 7 months of diabetes. Eye fundus and angiography images did not show any abnormalities in the retinal vasculature from the onset of diabetes to Month 7 as exemplified with selected examples shown in Figure 10. The assessment of the eye fundus of the retina revealed an abnormal vascular
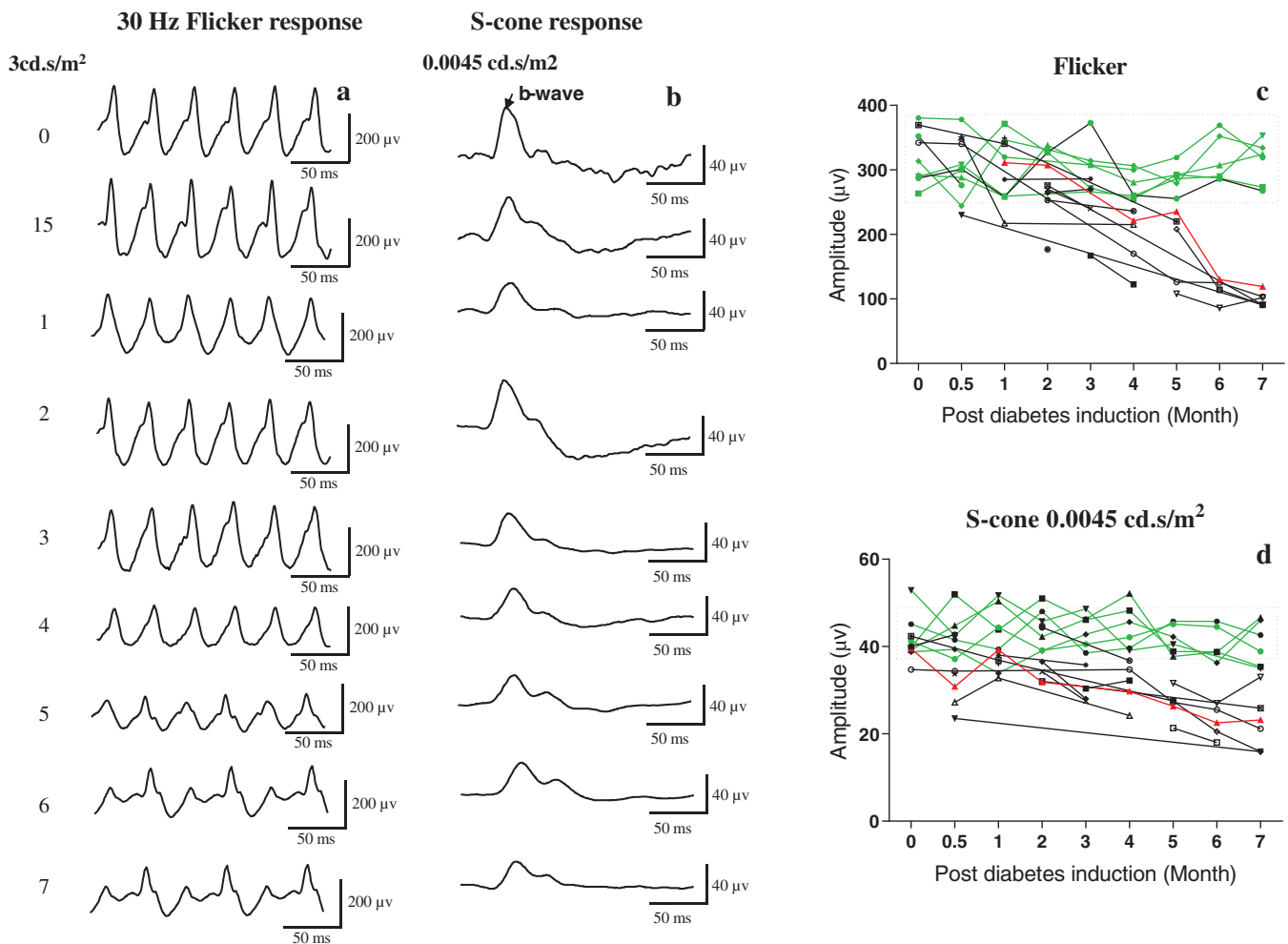
FIGURE 7 Photopic cone response at 3 cd.s/m^2 after 10 min light adaptation with 30 cd.s/m^2 background. (a–c) Flicker 30 Hz response. (b–d) Photopic S-cone response elicited at 0.0045 cd.s/m^2 in a red-orange background of 2.2 cd.s/m^2. (D) Diabetic: $n = 18$; (C) control: $n = 6$ (green curves) [Color figure can be viewed at wileyonlinelibrary.com]

architecture appeared at Months 6 and 7 (Figure 9). This vessel abnormality reflected by a retinal vessel tortuosity at Month 6. Also at Months 6 and 7, we noticed the appearance of exudates in the superior periphery of the retina in diabetic *P. obesus* (Figure 11(a)). These exudates were observed by OCT section in the superior retina (Figure 11(b); red arrows).

4 | DISCUSSION

Although DR in the diet-induced diabetes of *P. obesus* was previously described (Dellaa et al., 2018; T. Saidi et al., 2011). However, its onset and progression were never reported. The present study compared, for the first time, the evolution of retinal function with ERGs and clinical retinal imaging with OCT, FO, and angiography in adult *P. obesus* to assess whether, like in human, neuronal damage (especially early functional damage) precedes vascular alteration .

In a previous study, we showed that the ERG of *P. obesus* shares several features with that of human subjects (Dellaa et al., 2017)

making it a remarkable model to investigate the retinal complications of diet-induced type 2 DR. Moreover, *P. obesus* with type 2 DR develops early DR alteration at 3 months due to oxidative stress altering glutamate metabolism in connection with the activation of the glial cells (Baccouche et al., 2018). After 7 months under the same hypercaloric diet, these alterations become more prominent and now include vascular anomalies, elevated ratios of proangiogenic and anti-angiogenic growth factors and blood–retinal barrier breakdown, decreases in retinal cell layer thicknesses and density, accompanied by profound alterations in glia and reduction of the expression of short- and mid–/long-wavelength opsins (T. Saidi et al., 2011). In the present study, which followed the structural and functional alterations of the retina over a period of 7 months following the induction of diabetes, functional changes were detected as early as 2 months following the onset of DR compared to 6 months for the vascular changes.

We found that 3 months of diabetes in *P. obesus* did not affect the amplitude of the scotopic a-wave although a significant decrease in amplitude of the b-max, b-wave responses and mixed b-wave were noted. These results suggest that the rod bipolar cells, which are
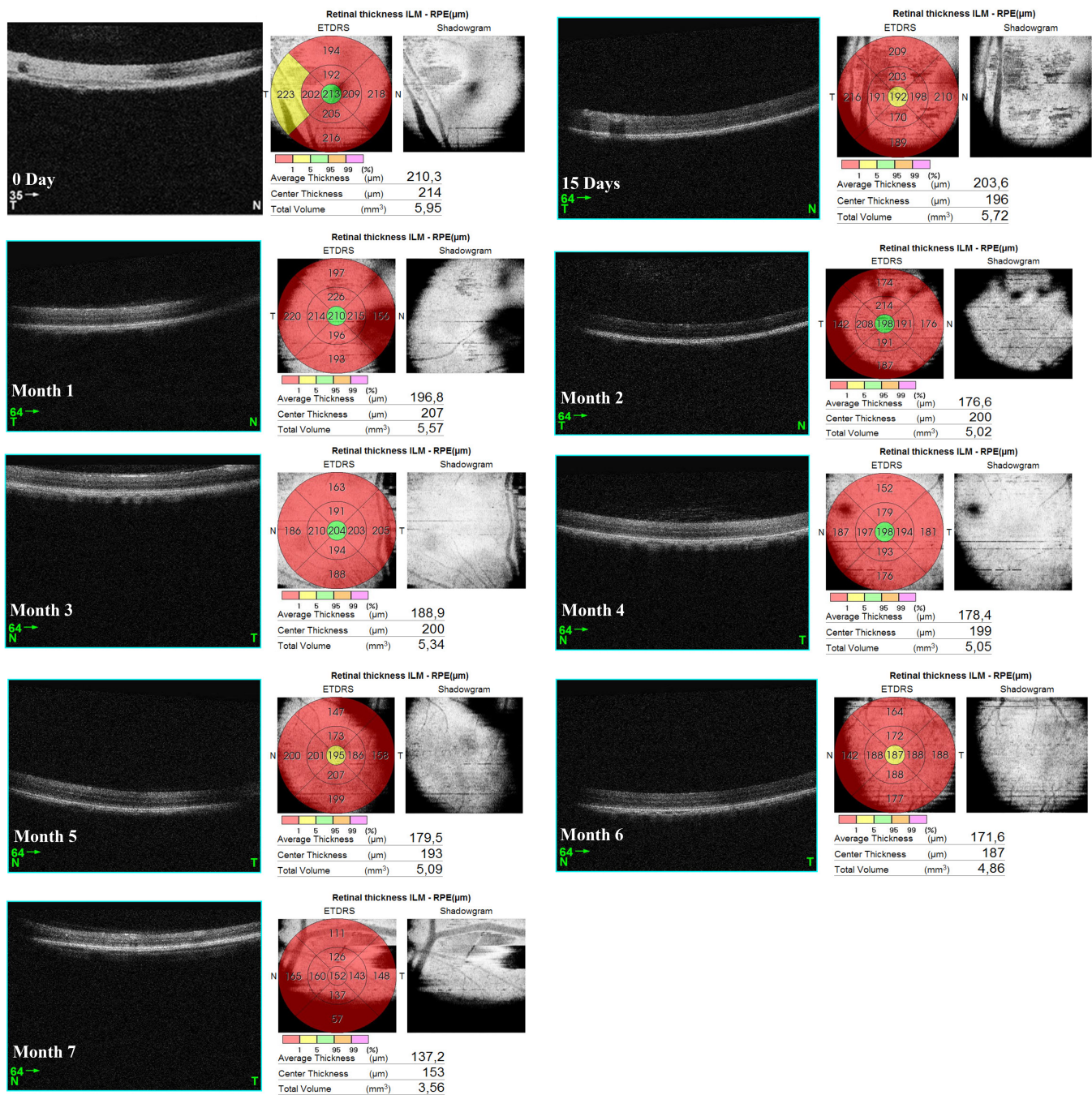
FIGURE 8 Ophthalmology examination in diabetic *Psammomys obesus*. Thickness analysis by OCT in diabetic *P. obesus* during 7 months of diabetes induction [Color figure can be viewed at wileyonlinelibrary.com]

involved in the genesis of the rod-mediated b-wave, were the first affected by the diabetes-induced retinopathy, a finding that confirms previous immunohistological report (Baccouche et al., 2018). Normal a-wave has been reported in diabetic humans with type 1 diabetes even without clinical signs, suggesting that Müller cell's reactivity and rod bipolar cells alteration symptoms (Lovasik & Kergoat, 1993) and treated Long-Evans rats (Hancock & Kraft, 2004; Ramsey et al., 2006). At the early stage of the disease (3 months) as in humans and the diabetic rat, the internal retina is the first affected, while there is no sign

of disorder noticed in the external retina and photoreceptors (T Saidi et al., 2012). The amplitude of the b-wave of the scotopic ERG is abnormal in diabetic patients that do not show clinical signs of DR (Coupland, 1987; Hardy et al., 1995). Unlike *Psammomys obesus* and human, another study showed that the amplitude of the a-wave was significantly reduced after 10–12 weeks of STZ induction in Sprague Dawley rats (Q. Li et al., 2002; Phipps et al., 2004). Furthermore, in diabetic high-fat diet-induced nocturnal rodent, *Meriones shawi* abnormalities of several ERG components were noticed under scotopic and

TABLE 2 Retinal thickness by optical coherence tomography

	Month 1		Month 2		Month 3		Month 4		Month 5		Month 6		Month 7	
	Control	Diabetic	Control	Diabetic	Control	Diabetic	Control	Diabetic	Control	Diabetic	Control	Diabetic	Control	Diabetic
Thickness (µm)	198.1 ± 0.6	182.37 ± 9.17	198.85 ± 2.05	192.4 ± 7.15	189.2 ± 14	181.25 ± 2.29	198.25 ± 6.05	181.37 ± 4.66	192.95 ± 4.05	181.7 ± 5.07	197.5 ± 10.3	179.56 ± 7.18	187.9 ± 5.5	139.1 ± 11.48
p-value	0.3		0.5		0.4		0.1		0.16		0.23		0.049 *	

Note: Data are expressed as the mean ± SEM. Thickness is in microvolts (µm).

*p ≤ .05.

photopic conditions at 3 months of diabetes induction, suggesting that rod and cone pathways are both susceptible to diabetes (Hammoum et al., 2018). The same results are shown in another HFD-induced obesity C57BL/6J mice (Chang et al., 2015).

A significant decrease in photopic a-wave precedes that of the b-wave. The b-wave reflects mainly the activity of the ON bipolar cells and Muller cells in adults pigmented rabbits (Dong & Hare, 2000). Early alterations in amplitude of the ERG b-wave and OPs were previously reported in several animal studies using experimentally induced diabetes (Q. Li et al., 2002; Ramsey et al., 2006). Ma et al. (Ma et al., 2009) reported a b-wave decrease 3 months following STZ-induced diabetes in Male Sprague–Dawley rats, Hancock and Kraft (Hancock & Kraft, 2004) reported that a b-wave decrease 12 weeks after STZ-injection in Long Evans. In contrast (Kohzaki et al., 2008), showed unaffected b-waves 11 weeks after STZ injection in Sprague–Dawley rats. No difference was detected in the photopic b/a-wave ratio during 6 months of the experiment in *P. obesus*, this fact shows that a- and b-waves are similarly decreased (Dellaa et al., 2018).

The amplitudes of the OPs were affected earlier than that of the a- and b-waves in diabetic *P. obesus*. Similar findings have also been reported by Kizawa et al. (2006) in patients with diabetes. In diabetic Sprague–Dawley rats animals, the OPs are affected much earlier (Bui et al., 2003) than outer retinal response (Kizawa et al., 2006; Phipps et al., 2004). In fact, alterations in oscillatory potentials have been shown to predict the onset of proliferative retinopathy better than vascular lesions seen on fundus photographs (Bresnick & Palta, 1987). In the present study, we observed an early amplitude decrease of scotopic OP2 1 month following the onset of diabetes compared to 3 months for photopic OP1 and OP2. Male Sprague–Dawley rats, under STZ treatment for 6 weeks, showed a decrease in scotopic OP1 and OP2 (Ishikawa et al., 1996). Similarly, in Long Evans rats treated with STZ for up to 12 weeks, only the OPs were affected, while no differences in the amplitude of the scotopic a- or b-waves were noted (Ramsey et al., 2006). In subjects with nonproliferative DR, the full field ERGs showed that the OPs (OP1-OP4) were significantly reduced in amplitude (Luu et al., 2010). It has been reported that the amplitude of the OPs is the best indicator of the severity of the diabetic retinopathy (Holopigian et al., 1997).

The PhNR, which reflects the contribution of ganglion cells in human (Colotto et al., 2000), was reduced by Month 4 in *P. obesus*, which is less sensitive than OPs. In human DR, it was reported that the amplitude of the PhNR was reduced along with the cone b-wave (Kizawa et al., 2006).

Given that the retinal function in *P. obesus*, as assessed with the ERG, was shown to share similarities with that of human (Dellaa et al., 2017; Dellaa et al., 2018), it would represent a unique model to test the preventive and curative effects of biomolecules, nutraceuticals, or biosimilar drugs depending on the evolution and classification of RD, which is a reversible pathology if the therapeutic management is done at an early stage for each cell type. The latter claim is strengthened by the fact that in our model, we observed that neuronal dysfunction as assessed with the ERG preceded by more
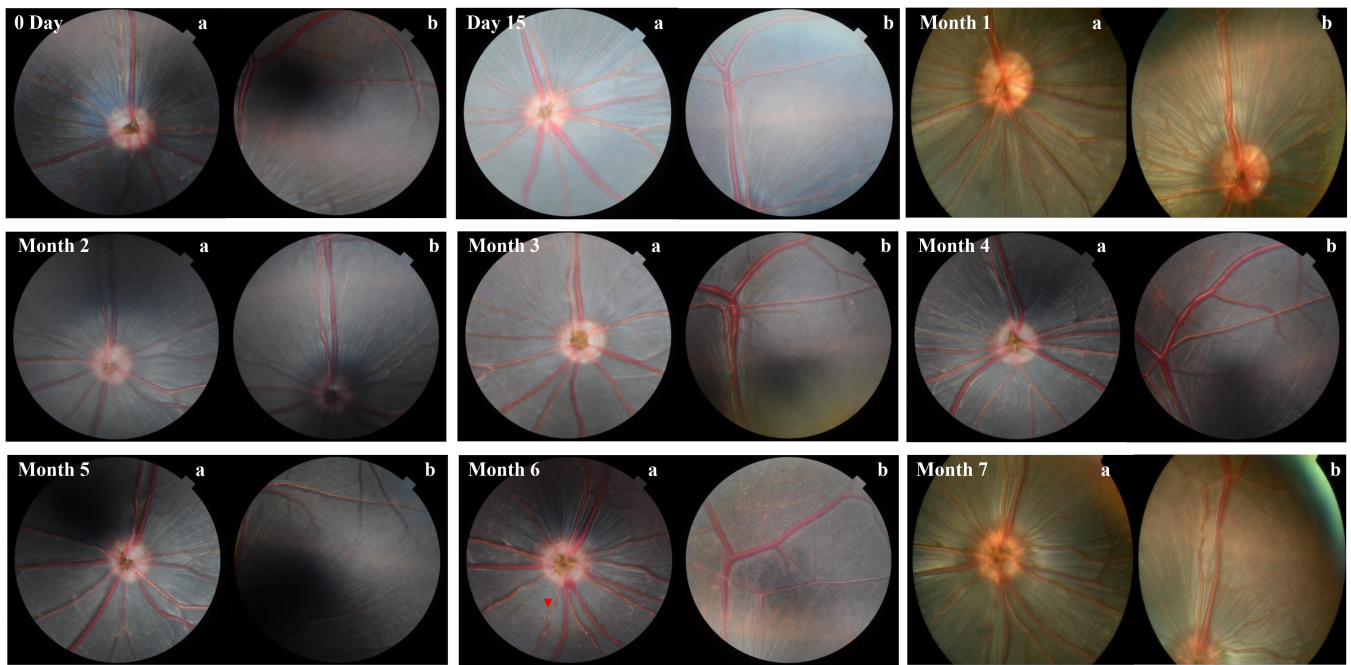
FIGURE 9 Ophthalmology examination in diabetic *P. obesus*. Eye fundus vasculature in the optic nerve (a) and visual streak (b) in diabetic *P. obesus* during 7 months of diabetes induction. Retinal vessel abnormality reflected by a retinal vessel tortuosity (red arrow) [Color figure can be viewed at wileyonlinelibrary.com]
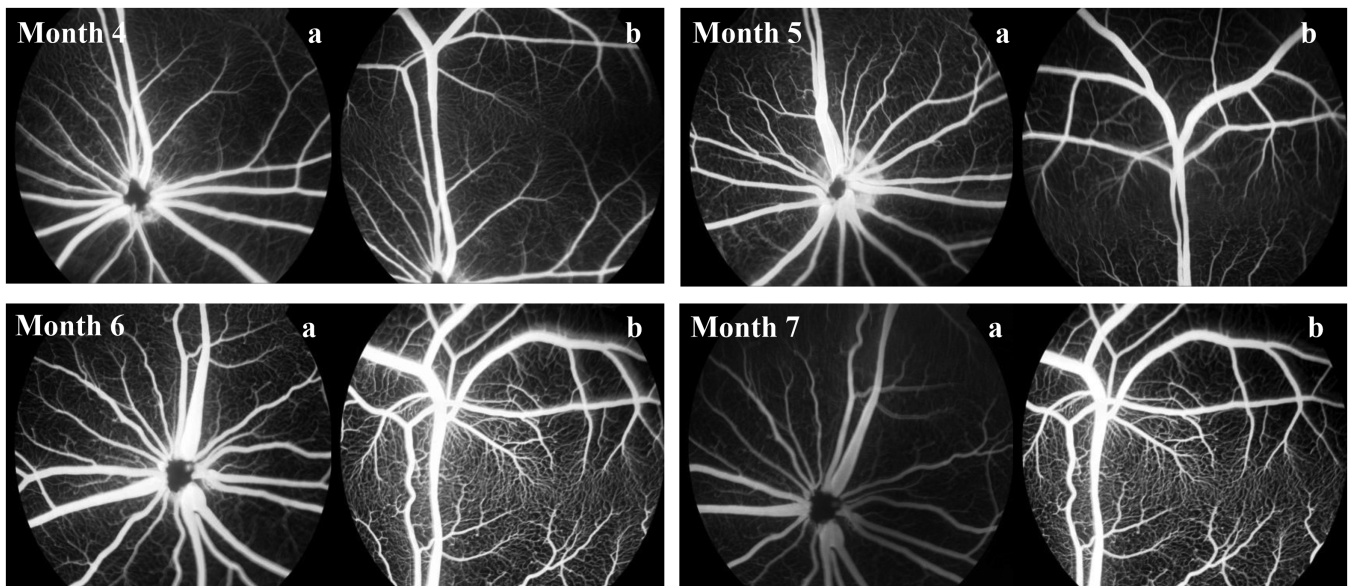

FIGURE 10 Ophthalmology examination in diabetic *Psammomys obesus*. Angiography in the optic nerve (a) and visual streak (b), in diabetic *P. obesus* during 7 months of diabetes induction

than 5 months the vascular changes as assessed with ophthalmoscopy, findings that are with those previously published by (Brunette & Lafond, 1983) on human diabetic patients.

The clinical diagnosis of DR relies primarily on the detection of vascular lesions at fundus examination. The retinal fundus reflects the structural integrity of the retinal vascular system. In the present study, fundus pictures disclosed an intact vasculature for the first 5 months

following the induction of diabetes, while at 6 months, we observed the first signs of diabetes namely, lipid exudates and tortuous blood vessels appearing in the superior retina. In contrast, functional impairment appeared after 1 month for scotopic ERG (OP1) and after 3 months for photopic OP1 and OP2. It was also previously demonstrated in Ins2 (Akita) mice that clinical correlates of human diabetic retinopathy are absent up to 6 months of age; no vascular changes
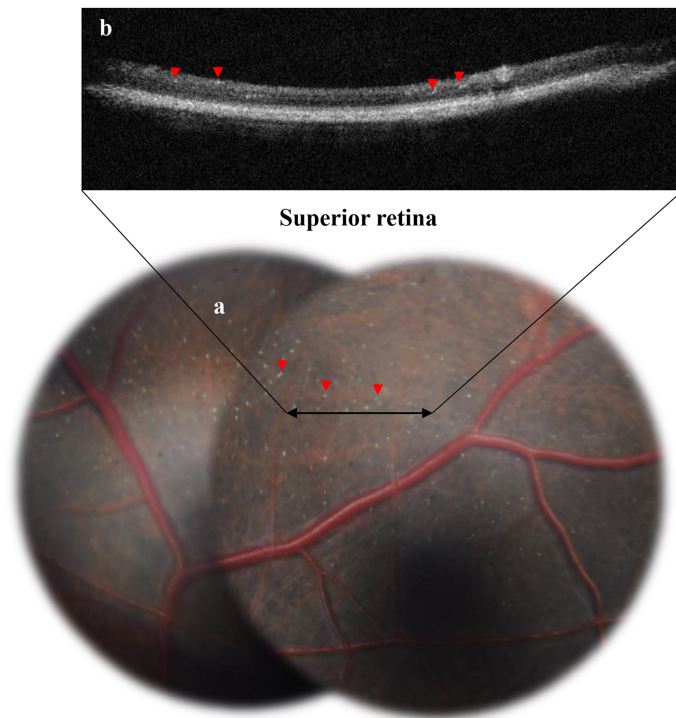
FIGURE 11 Peripheral retinal alterations after 6 months of diabetes in *P. obesus*. Fundus (a) and OCT (b) images showed vascular abnormalities with the presence of exudates (red arrows) in the superior periphery retina [Color figure can be viewed at wileyonlinelibrary.com]

were detected by fluorescein angiography or by scanning laser ophthalmoscopy (McLenachan et al., 2013). Another study on rats (SHR/N-cp; a model of T2D also reported the absence of retinal vascular alterations by fluorescein angiography and ophthalmoscopic exudates after 4 and 8 months of age (M. Huber et al., 2011). However, significant vascular alteration such as microaneurysm, leaky capillaries, venous beading, tortuous vessels, capillary dropouts, and attenuation of vessels were observed in Kimba and Akimba mice (Rakoczy et al., 2010). In streptozotocin-induced diabetic rats, the first macrovascular alterations observed with fluorescein angiography (dilation of venules and arterioles) only occurred after 24 weeks of diabetes (Kumar Gupta et al., 2013).

It has been reported that the retinal pigment epithelium (RPE) contributes components to the ERG (Steinberg et al., 1985). The breakdown of the endothelial barrier in DR has been investigated extensively. There is evidence that the RPE is also affected in diabetes, and changes in its electrical resistance will change the amplitude of components generated in the retina (Steinberg et al., 1985).

Clinical analysis of retinal thickness by OCT has shown a decrease of retinal thickness by Month 7. Chen et al. (Hombrebueno et al., 2014) revealed a progressive thinning of the retina from 3 months in diabetic retinal in the Ins2Akita mouse, while no fundus lesions were detected in the fundus imaging such microaneurysm and exudates up to 9 months. Few studies using OCT are performed on animal models and compared against data related to clinical research on humans. The OCT examination performed in patients with type

1 and 2 diabetes showed a decrease in the thickness of the inner layers of the retina, which is weakly associated with vascular lesions (Chhablani et al., 2015; van Dijk et al., 2009; van Dijk et al., 2010; van Dijk et al., 2012). A 5% decrease in retinal thickness has been estimated in diabetic patients with clinically significant reduction in retinal function (Biallosterski et al., 2007). Moreover, *P. obesus* also has shown the existence of a horizontal visual streak-like pattern region with the absence of larger blood vessels, which is also described in our laboratory in *Meriones shawi* (Hammoum et al., 2017) and assessed in other rodents(G. Huber et al., 2010). This visual streak-like pattern region rich in cones is the equivalent to the human macula and may be interesting to be studied in depth for more functional information on the central retina of humans. In summary, we showed for the first time the progression of diabetic retinopathy in diet-induced diabetes *P. obesus* at the functional and morphological level.

5 | CONCLUSION

As in human, in the early stages of diabetes, measurement of retinal function with the ERG is more sensitive compared with morphological detection of lesions and the oscillatory potentials are the earliest affected components following diet-induced diabetes. *P. obesus* is an excellent model to study the genesis of the disease "diabetic retinopathy" and testing the biomolecules of preventive and therapeutic effects in the agri-food and pharmaceutical industries.

AUTHORS CONTRIBUTION

Ahmed Dellaa: Writing – Original Draft Preparation, Project Administration, Resources, formal analysis data. **Sihem Mbarek:** Conceptualization & Editing. **Rim Kahloun**: Methodology; Validation. **Mohamed Dogui**: Resources; Software. **Moncef Khairallah**: Resources; Software. **Imane Hammoum**: Investigation – Technical assistance for experimentation. **Narjess Ben Rayana-Chekir**: Resources. **Ridha Charfeddine**: Supervision; Funding Acquisition. **Pierre Lachapelle**: Writing – Visualization – Review & Editing. **Rafika Ben Chaouacha-Chekir**: Conceptualization, Investigation; Project Administration, Resources; Visualization – Writing – Review & Editing – Funding Acquisition.

PEER REVIEW

The peer review history for this article is available at https://publons.com/publon/10.1002/cne.25114.

DATA AVAILABILITY STATEMENT

ORCID

Rafika Ben Chaouacha-Chekir ⓘ https://orcid.org/0000-0002-3121-2191

REFERENCES

Abu-El-Asrar, A. M., Dralands, L., Missotten, L., Al-Jadaan, I. A., & Geboes, K. (2004). Expression of apoptosis markers in the retinas of human subjects with diabetes. *Investigative Ophthalmology & Visual Science*, 45(8), 2760–2766. https://doi.org/10.1167/iovs.03-1392

Aiello, L. P., Gardner, T. W., King, G. L., Blankenship, G., Cavallerano, J. D., Ferris, F. L., 3rd, & Klein, R. (1998). Diabetic retinopathy. *Diabetes Care*, 21(1), 143–156.

Baccouche, B., Benlarbi, M., Barber, A. J., & Ben Chaouacha-Chekir, R. (2018). Short-term Administration of Astaxanthin Attenuates Retinal Changes in diet-induced diabetic *Psammomys obesus*. *Current Eye Research*, 43(9), 1177–1189. https://doi.org/10.1080/02713683.2018.1484143

Barber, A. J., Lieth, E., Khin, S. A., Antonetti, D. A., Buchanan, A. G., & Gardner, T. W. (1998). Neural apoptosis in the retina during experimental and human diabetes. Early onset and effect of insulin. *The Journal of Clinical Investigation*, 102(4), 783–791. https://doi.org/10.1172/JCI2425

Bearse, M. A., Han, Y., Schneck, M. E., Barez, S., Jacobsen, C., & Adams, A. J. (2004). Local multifocal oscillatory potential abnormalities in diabetes and early diabetic retinopathy. *Investigative Ophthalmology & Visual Science*, 45(9), 3259–3265. https://doi.org/10.1167/iovs.04-0308

Biallosterski, C., van Velthoven, M. E., Michels, R. P., Schlingemann, R. O., DeVries, J. H., & Verbraak, F. D. (2007). Decreased optical coherence tomography-measured pericentral retinal thickness in patients with diabetes mellitus type 1 with minimal diabetic retinopathy. *The British Journal of Ophthalmology*, 91(9), 1135–1138. https://doi.org/10.1136/bjo.2006.111534

Bresnick, G. H., & Palta, M. (1987). Predicting progression to severe proliferative diabetic retinopathy. *Archives of Ophthalmology*, 105(6), 810–814.

Brunette, J. R., & Lafond, G. (1983). Electroretinographic evaluation of diabetic retinopathy: Sensitivity of amplitude and time of response. *Canadian Journal of Ophthalmology*, 18(6), 285–289.

Bui, B. V., Armitage, J. A., Tolcos, M., Cooper, M. E., & Vingrys, A. J. (2003). ACE inhibition salvages the visual loss caused by diabetes. *Diabetologia*, 46(3), 401–408. https://doi.org/10.1007/s00125-003-1042-7

Chang, R. C., Shi, L., Huang, C. C., Kim, A. J., Ko, M. L., Zhou, B., & Ko, G. Y. (2015). High-fat diet-induced retinal dysfunction. *Investigative Ophthalmology & Visual Science*, 56(4), 2367–2380. https://doi.org/10.1167/iovs.14-16143

Chhablani, J., Sharma, A., Goud, A., Peguda, H. K., Rao, H. L., Begum, V. U., & Barteselli, G. (2015). Neurodegeneration in type 2 diabetes: Evidence from spectral-domain optical coherence tomography. *Investigative Ophthalmology & Visual Science*, 56(11), 6333–6338. https://doi.org/10.1167/iovs.15-17334

Colotto, A., Falsini, B., Salgarello, T., Iarossi, G., Galan, M. E., & Scullica, L. (2000). Photopic negative response of the human ERG: Losses associated with glaucomatous damage. *Investigative Ophthalmology & Visual Science*, 41(8), 2205–2211.

Coupland, S. G. (1987). A comparison of oscillatory potential and pattern electroretinogram measures in diabetic retinopathy. *Documenta Ophthalmologica*, 66(3), 207–218.

Cunha-Vaz, J., Faria de Abreu, J. R., & Campos, A. J. (1975). Early breakdown of the blood-retinal barrier in diabetes. *The British Journal of Ophthalmology*, 59(11), 649–656.

Dellaa, A., Benlarbi, M., Hammoum, I., Gammoudi, N., Dogui, M., Messaoud, R., … Ben Chaouacha-Chekir, R. (2018). Electroretinographic evidence suggesting that the type 2 diabetic retinopathy of the sand rat *Psammomys obesus* is comparable to that of humans. *PLoS One*, 13(2), e0192400. https://doi.org/10.1371/journal.pone.0192400

Dellaa, A., Polosa, A., Mbarek, S., Hammoum, I., Messaoud, R., Amara, S., Azaiz, R., Charfeddine, R., Dogui, M., Khairallah, M., Lachapelle, P., & Ben Chaouacha-Chekir, R. (2017). Characterizing the retinal function of *Psammomys obesus*: A diurnal rodent model to study human retinal function. *Current Eye Research*, 42(1), 79–87. https://doi.org/10.3109/02713683.2016.1141963

Dellaa, A., Polosa, A., Mbarek, S., Hammoum, I., Messaoud, R., Amara, S., … Ben Chaouacha-Chekir, R. (2016). Characterizing the retinal function of *Psammomys obesus*: A diurnal rodent model to study human retinal function. *Current Eye Research*, 42, 1–9. https://doi.org/10.3109/02713683.2016.1141963

Dong, C. J., & Hare, W. A. (2000). Contribution to the kinetics and amplitude of the electroretinogram b-wave by third-order retinal neurons in the rabbit retina. *Vision Research*, 40(6), 579–589.

Fortune, B., Schneck, M. E., & Adams, A. J. (1999). Multifocal electroretinogram delays reveal local retinal dysfunction in early diabetic retinopathy. *Investigative Ophthalmology & Visual Science*, 40(11), 2638–2651.

Gotoh, Y., Machida, S., & Tazawa, Y. (2004). Selective loss of the photopic negative response in patients with optic nerve atrophy. *Archives of Ophthalmology*, 122(3), 341–346. https://doi.org/10.1001/archopht.122.3.341

Haines, H., Hackel, D. B., & Schmidt-Nielsen, K. (1965). Experimental diabetes mellitus induced by diet in the sand rat. *The American Journal of Physiology*, 208, 297–300. https://doi.org/10.1152/ajplegacy.1965.208.2.297

Hammoum, I., Benlarbi, M., Dellaa, A., Kahloun, R., Messaoud, R., Amara, S., Azaiz, R., Charfeddine, R., Dogui, M., Khairallah, M., Lukáts, Á., & Ben Chaouacha-Chekir, R. (2018). Retinal dysfunction parallels morphologic alterations and precede clinically detectable vascular alterations in *Meriones shawi*, a model of type 2 diabetes. *Experimental Eye Research*, 176, 174–187. https://doi.org/10.1016/j.exer.2018.07.007

Hammoum, I., Benlarbi, M., Dellaa, A., Szabo, K., Dekany, B., Csaba, D., … Benchouacha-Chekir, R. (2017). Study of retinal neurodegeneration and maculopathy in diabetic *Meriones shawi*: A particular animal model with human-like macula. *The Journal of Comparative Neurology*, 525, 2890–2914. https://doi.org/10.1002/cne.24245

Hancock, H. A., & Kraft, T. W. (2004). Oscillatory potential analysis and ERGs of normal and diabetic rats. *Investigative Ophthalmology & Visual Science*, 45(3), 1002–1008.

Hardy, K. J., Fisher, C., Heath, P., Foster, D. H., & Scarpello, J. H. (1995). Comparison of colour discrimination and electroretinography in evaluation of visual pathway dysfunction in aretinopathic IDDM patients. *The British Journal of Ophthalmology*, 79(1), 35–37. https://doi.org/10.1136/bjo.79.1.35

Hardy, K. J., Lipton, J., Scase, M. O., Foster, D. H., & Scarpello, J. H. (1992). Detection of colour vision abnormalities in uncomplicated type 1 diabetic patients with angiographically normal retinas. *The British Journal of Ophthalmology*, 76(8), 461–464.

Heng, L. Z., Comyn, O., Peto, T., Tadros, C., Ng, E., Sivaprasad, S., & Hykin, P. G. (2013). Diabetic retinopathy: Pathogenesis, clinical grading, management and future developments. *Diabetic Medicine*, 30(6), 640–650. https://doi.org/10.1111/dme.12089

Holm, K., Larsson, J., & Lovestam-Adrian, M. (2007). In diabetic retinopathy, foveal thickness of 300 mum seems to correlate with functionally significant loss of vision. *Documenta Ophthalmologica*, 114(3), 117–124. https://doi.org/10.1007/s10633-006-9044-7

Holopigian, K., Greenstein, V. C., Seiple, W., Hood, D. C., & Carr, R. E. (1997). Evidence for photoreceptor changes in patients with diabetic retinopathy. *Investigative Ophthalmology & Visual Science*, *38*(11), 2355–2365.

Hombrebueno, J. R., Chen, M., Penalva, R. G., & Xu, H. (2014). Loss of synaptic connectivity, particularly in second order neurons is a key feature of diabetic retinal neuropathy in the Ins2Akita mouse. *PLoS One*, *9*(5), e97970. https://doi.org/10.1371/journal.pone.0097970

Huber, G., Heynen, S., Imsand, C., vom Hagen, F., Muehlfriedel, R., Tanimoto, N., Feng, Y., Hammes, H.-P., Grimm, C., Peichl, L., Seeliger, M. W., & Beck, S. C. (2010). Novel rodent models for macular research. *PLoS One*, *5*(10), e13403.

Huber, M., Heiduschka, P., Ziemssen, F., Bolbrinker, J., & Kreutz, R. (2011). Microangiopathy and visual deficits characterize the retinopathy of a spontaneously hypertensive rat model with type 2 diabetes and metabolic syndrome. *Hypertension Research*, *34*(1), 103–112. https://doi.org/10.1038/hr.2010.168

Ishikawa, A., Ishiguro, S., & Tamai, M. (1996). Changes in GABA metabolism in streptozotocin-induced diabetic rat retinas. *Current Eye Research*, *15*(1), 63–71.

Kaiser, N., Nesher, R., Donath, M. Y., Fraenkel, M., Behar, V., Magnan, C., Ktorza, A., Cerasi, E., & Leibowitz, G. (2005). *Psammomys obesus*, a model for environment-gene interactions in type 2 diabetes. *Diabetes*, *54*(Suppl 2), S137–S144. https://doi.org/10.2337/diabetes.54.suppl_2.s137

Kizawa, J., Machida, S., Kobayashi, T., Gotoh, Y., & Kurosaka, D. (2006). Changes of oscillatory potentials and photopic negative response in patients with early diabetic retinopathy. *Japanese Journal of Ophthalmology*, *50*(4), 367–373. https://doi.org/10.1007/s10384-006-0326-0

Kohzaki, K., Vingrys, A. J., & Bui, B. V. (2008). Early inner retinal dysfunction in streptozotocin-induced diabetic rats. *Investigative Ophthalmology & Visual Science*, *49*(8), 3595–3604. https://doi.org/10.1167/iovs.08-1679

Kumar Gupta, S., Kumar, B., Srinivasan, B. P., Nag, T. C., Srivastava, S., Saxena, R., & Aggarwal, A. (2013). Retinoprotective effects of *Moringa oleifera* via antioxidant, anti-inflammatory, and anti-angiogenic mechanisms in streptozotocin-induced diabetic rats. *Journal of Ocular Pharmacology and Therapeutics*, *29*(4), 419–426. https://doi.org/10.1089/jop.2012.0089

Li, B., Barnes, G. E., & Holt, W. F. (2005). The decline of the photopic negative response (PhNR) in the rat after optic nerve transection. *Documenta Ophthalmologica*, *111*, 23–31. https://doi.org/10.1007/s10633-005-2629-8

Li, Q., Zemel, E., Miller, B., & Perlman, I. (2002). Early retinal damage in experimental diabetes: Electroretinographical and morphological observations. *Experimental Eye Research*, *74*(5), 615–625. https://doi.org/10.1006/exer.2002.1170

Lovasik, J. V., & Kergoat, H. (1993). Electroretinographic results and ocular vascular perfusion in type 1 diabetes. *Investigative Ophthalmology & Visual Science*, *34*(5), 1731–1743.

Luu, C. D., Szental, J. A., Lee, S. Y., Lavanya, R., & Wong, T. Y. (2010). Correlation between retinal oscillatory potentials and retinal vascular caliber in type 2 diabetes. *Investigative Ophthalmology & Visual Science*, *51*(1), 482–486. https://doi.org/10.1167/iovs.09-4069

Ma, P., Luo, Y., Zhu, X., Ma, H., Hu, J., & Tang, S. (2009). Phosphomannopentaose sulfate (PI-88) inhibits retinal leukostasis in diabetic rat. *Biochemical and Biophysical Research Communications*, *380*(2), 402–406. https://doi.org/10.1016/j.bbrc.2009.01.092

McCulloch, D. L., Marmor, M. F., Brigell, M. G., Hamilton, R., Holder, G. E., Tzekov, R., & Bach, M. (2015). ISCEV standard for full-field clinical electroretinography (2015 update). *Documenta Ophthalmologica*, *130*(1), 1–12. https://doi.org/10.1007/s10633-014-9473-7

McLenachan, S., Chen, X., McMenamin, P. G., & Rakoczy, E. P. (2013). Absence of clinical correlates of diabetic retinopathy in the Ins2Akita

retina. *Clinical & Experimental Ophthalmology*, *41*(6), 582–592. https://doi.org/10.1111/ceo.12084

Nentwich, M. M., & Ulbig, M. W. (2015). Diabetic retinopathy - ocular complications of diabetes mellitus. *World Journal of Diabetes*, *6*(3), 489–499. https://doi.org/10.4239/wjd.v6.i3.489

Palmowski, A. M., Sutter, E. E., Bearse, M. A., & Fung, W. (1997). Mapping of retinal function in diabetic retinopathy using the multifocal electroretinogram. *Investigative Ophthalmology & Visual Science*, *38*(12), 2586–2596.

Phipps, J. A., Fletcher, E. L., & Vingrys, A. J. (2004). Paired-flash identification of rod and cone dysfunction in the diabetic rat. *Investigative Ophthalmology & Visual Science*, *45*(12), 4592–4600. https://doi.org/10.1167/iovs.04-0842

Rakoczy, E. P., Ali Rahman, I. S., Binz, N., Li, C. R., Vagaja, N. N., de Pinho, M., & Lai, C. M. (2010). Characterization of a mouse model of hyperglycemia and retinal neovascularization. *The American Journal of Pathology*, *177*(5), 2659–2670. https://doi.org/10.2353/ajpath.2010.090883

Ramsey, D. J., Ripps, H., & Qian, H. (2006). An electrophysiological study of retinal function in the diabetic female rat. *Investigative Ophthalmology & Visual Science*, *47*(11), 5116–5124. https://doi.org/10.1167/iovs.06-0364

Rangaswamy, N. V., Frishman, L. J., Dorotheo, E. U., Schiffman, J. S., Bahrani, H. M., & Tang, R. A. (2004). Photopic ERGs in patients with optic neuropathies: Comparison with primate ERGs after pharmacologic blockade of inner retina. *Investigative Ophthalmology & Visual Science*, *45*(10), 3827–3837. https://doi.org/10.1167/iovs.04-0458

Rosolen, S. G., Rigaudiere, F., LeGargasson, J. F., Chalier, C., Rufiange, M., Racine, J., Joly, S., & Lachapelle, P. (2004). Comparing the photopic ERG i-wave in different species. *Veterinary Ophthalmology*, *7*(3), 189–192. https://doi.org/10.1111/j.1463-5224.2004.04022.x

Saidi, T., Chaouacha-Chekir, R., & Hicks, D. (2012). Advantages of *Psammomys obesus* as an animal model to study diabetic retinopathy. *Journal of Diabetes and Metabolism*, *3*(207), 2.

Saidi, T., Mbarek, S., Omri, S., Behar-Cohen, F., Chaouacha-Chekir, R. B., & Hicks, D. (2011). The sand rat, *Psammomys obesus*, develops type 2 diabetic retinopathy similar to humans. *Investigative Ophthalmology & Visual Science*, *52*(12), 8993–9004. https://doi.org/10.1167/iovs.11-8423

Schmidt-Nielsen, K., Haines, H. B., & Hackel, D. B. (1964). Diabetes mellitus in the sand rat induced by standard laboratory diets. *Science*, *143*(3607), 689–690. https://doi.org/10.1126/science.143.3607.689

Shirao, Y., & Kawasaki, K. (1998). Electrical responses from diabetic retina. *Progress in Retinal and Eye Research*, *17*(1), 59–76.

Steinberg, R. H., Linsenmeier, R. A., & Griff, E. R. (1985). Chapter 2 retinal pigment epithelial cell contributions to the electroretinogram and electrooculogram. *Progress in Retinal Research*, *4*, 33–66. https://doi.org/10.1016/0278-4327(85)90004-5

Sugimoto, M., Sasoh, M., Ido, M., Wakitani, Y., Takahashi, C., & Uji, Y. (2005). Detection of early diabetic change with optical coherence tomography in type 2 diabetes mellitus patients without retinopathy. *Ophthalmologica*, *219*(6), 379–385. https://doi.org/10.1159/000088382

van Dijk, H. W., Kok, P. H., Garvin, M., Sonka, M., Devries, J. H., Michels, R. P., van Velthoven, M. E. J., Schlingemann, R. O., Verbraak, F. D., & Abramoff, M. D. (2009). Selective loss of inner retinal layer thickness in type 1 diabetic patients with minimal diabetic retinopathy. *Investigative Ophthalmology & Visual Science*, *50*(7), 3404–3409. https://doi.org/10.1167/iovs.08-3143

van Dijk, H. W., Verbraak, F. D., Kok, P. H., Garvin, M. K., Sonka, M., Lee, K., DeVries, J. H., Michels, R. P. J., van Velthoven, M. E. J., Schlingemann, R. O., & Abramoff, M. D. (2010). Decreased retinal ganglion cell layer thickness in patients with type 1 diabetes. *Investigative Ophthalmology & Visual Science*, *51*(7), 3660–3665. https://doi.org/10.1167/iovs.09-5041

van Dijk, H. W., Verbraak, F. D., Kok, P. H., Stehouwer, M., Garvin, M. K., Sonka, M., DeVries, J. H., Schlingemann, R. O., & Abramoff, M. D.

(2012). Early neurodegeneration in the retina of type 2 diabetic patients. *Investigative Ophthalmology & Visual Science*, *53*(6), 2715–2719. https://doi.org/10.1167/iovs.11-8997

Verma, A., Raman, R., Vaitheeswaran, K., Pal, S. S., Laxmi, G., Gupta, M., Shekar, S. C., & Sharma, T. (2012). Does neuronal damage precede vascular damage in subjects with type 2 diabetes mellitus and having no clinical diabetic retinopathy? *Ophthalmic Research*, *47*(4), 202–207. https://doi.org/10.1159/000333220

Viswanathan, S., Frishman, L. J., Robson, J. G., & Walters, J. W. (2001). The photopic negative response of the flash electroretinogram in primary open angle glaucoma. *Investigative Ophthalmology & Visual Science*, *42*(2), 514–522.

Wachtmeister, L. (1998). Oscillatory potentials in the retina: What do they reveal. *Progress in Retinal and Eye Research*, *17*(4), 485–521.